Influence of Physical Cross-links in Amorphous PET on Room Temperature Ageing

Z. Kiflie, S. Piccarolo, E. Vassileva§*

piccarolo@unipa.it, Dip. Ingegneria Chimica, Viale delle Scienze, 90128 Palermo, Italy
§ Universitat Kaiserslautern, Institut für Verbundwerkstoffe GmbH, Erwin Schrodinger Strasse Geb.58, D-67663 Kaiserslautern, Germany

Summary: Physical cross-links arise in amorphous PET upon solidification from the melt, their size distribution depending on the cooling rate adopted during a CCT (Continuous Cooling Transformation). They form a fading network structure. Above the T_g, their stability decreases with temperature. Physical cross-links stable above the T_g can influence the nucleation rate. Ageing, below T_g, is also affected by cooling rate and therefore by physical cross-links. However upon ageing new physical cross-links arise although their size and stability continue to depend on cooling rate.

Introduction

Processing of slowly crystallizing polymers like poly(ethylene terephthalate) PET as in reheat stretch blow moulding of bottles, heat setting, production of films and fibers, etc. is usually accomplished from the amorphous state. The properties of the starting amorphous polymer, therefore, will directly or indirectly influence the physical and mechanical properties of such products.

We have recently shown that a Continuous Cooling Transformation (CCT) procedure can be used to simulate the cooling conditions employed during processing from the melt and therefore the structure developed [1]. According to this procedure, amorphous PET is formed in a wide latitude of cooling rates spanning from ca 2°C/s, depending on the molecular weight, up to ca 7000°C/s (the highest cooling rates achieved). Below 2°C/s the CCT of PET gives rise to the triclinic phase with a mechanism where secondary crystallization is increasingly important for lower cooling rates. The formation of a phase of intermediate order, defined as a precrystalline phase, in the amorphous cooling rate range has also been postulated [2].

The exact nature of this phase is not known. It is neither crystalline nor amorphous since the evidence summarized in the following paragraph cannot be reconciled with any of

 CCC 1022-1360/00/$ 17.50+.50/0

the two. However, microhardness measurements show that this state of intermediate order affects mechanical properties. This may be explained if one thinks of crystalline clusters of intermediate order dispersed in the amorphous polymer. Nevertheless, many questions arise about their influence on the behavior of the material below the glass transition temperature (T_g) during ageing and above the T_g during crystallization from the glass. As for the latter we have recently studied the influence of cooling rate, and therefore of the physical cross-links, on the crystallization from the glass [3].

The amorphous phase is indeed a glass at room temperature and it is reasonable to think that the excess free volume frozen during quenching may provide sufficient space for local mobility in such a way as to determine the onset of crystalline clusters at some stage of the solidification process. So far, there are only conflicting evidences on this possibility in the literature and it should be emphasized that these arguments are just only speculations. As an extreme example, the evidence about the possibility of glassy PET to crystallize even below T_g under an applied suitable stress state may be cited [4].

The subject is certainly complicated and the stability of physical cross-links cannot be treated only by equilibrium thermodynamics arguments. It is not known, for instance, whether the physical cross-links could be identified as a true mesomorphic phase [5]. The coherence of the concept of paracrystallinity[6] is not clear since a paracrystal is defective per se and its stability does not necessarily depend on external constraints. Such constraints, which play a significant role on the departure from equilibrium, may depend not only on the frozen-in cooperative motions in the glassy state but also on the physical cross-links themselves as the latter can act as obstacles to the elementary motions. Furthermore, the relationship of physical cross-links with the so called rigid amorphous phase, frequently reported in semicrystalline PET [7-9] is not clear.

Physical cross-links, as intended here, have also been inductively identified by other authors under different circumstances. Imai et al[10] have given experimental evidence of a spontaneous nematic transition in PET already postulated by Doi et al[11] on rigid chain polymers. On the basis of SANS experiments at 88°C a transition was observed to take place by spinodal decomposition at the early stages of crystallization due to the increase of trans conformations of the ethylene moieties. Fukao et al.[12] have shown the onset of an α' relaxation prior to the crystallization of PET by dielectric spectroscopy. Qian[13] has extensively studied the conformational changes occurring in different polymers by FTIR. He postulated the occurrence of cohesional entanglements which,

according to him, arise if sufficient free volume is frozen upon quenching from above the T_g. They are however unstable and sub-T_g annealing would cancel their effect. His viewpoint is different from the previous authors since it assumes that the cohesional entanglements arise due to the energy driven spontaneous self assembly of chain segments. The nematic transition observed by Imai and also the α' relaxation observed by Fukao may presumably arise simply due to short range interactions and therefore due to chain rigidity.

Other works have observed the influences of physical cross-links on the crystallization behavior and on the properties of the amorphous phase. Ageing was shown to enhance crystallization above T_g thus invoking an increase of nucleation density in the amorphous polymer [14]. This behavior has been recently disputed since a maximum of crystallization rate vs. ageing time was observed and interpreted as the coexistence of two opposing mechanisms: a decrease of mobility should indeed take place for long ageing times[15].

In this work we first examine how the features of the precrystalline phase depend on the solidification conditions and then relate these features to the room temperature ageing behavior as a function of the cooling rate employed for sample preparation. This is made possible by the unique Continuous Cooling Transformation (CCT) approach, which allows to control the morphology developed. Thus, although the initial state of the samples cannot be identified by state variables as its departure from equilibrium is unknown, cooling rate is used here as a parameter identifying such departure. Therefore, we can associate the previously identified precrystalline phase with physical cross-links.

Experimental

The materials used were a PET resin (IV =0.62 dl/g, Mw=39000) kindly supplied by Mossi & Ghisolfi Group and a commercial extrusion grade PMMA. PET was dried at 170°C for 7 hrs in vacuum. Films of ca 200μm were also prepared in vacuum by compression molding of the dried pellets.

Details on the experimental CCT approach have been reported previously [2]. A systematic analysis of the heat transfer conditions necessary for obtaining a homogeneous sample has also been examined [16]. In this approach samples of PET are first held in the melt at 280°C for 5min in a nitrogen ambient and afterwards quenched to ca 0°C by spraying a cooling fluid while recording the temperature history. Desired

cooling rates are obtained by a proper choice of the cooling fluid (water or air) and its flow rate. Cooling rates ranging from 2 to well above 1000°C/s were used to prepare apparently amorphous samples, (see Fig. 1). PMMA samples were also obtained with the same procedure although only one cooling rate, of ca 10°C/s was adopted.

A gradient column filled with a solution of n-heptane and carbon tetrachloride having a resolution of 0.0001 kg/L and a repeatability within 0.0002 kg/L was used for density measurement at 25°C. Each sample was properly checked against entrapped air bubbles using a microscope and afterwards degassed before being introduced into the column. An average of five samples were analysed for each test condition.

Microhardness measurements were carried out using an MHT-10 Vickers indenter by Anton Paar. Peak forces of 0.1, 0.15 and 0.25 N were used to correct for instantaneous elastic recovery [11] and an average of five measurements were done with each force. The microhardness was calculated from the residual projected indented area using the relation:

$$MH = 2F\frac{\sin(\alpha/2)}{d^2} = 1.854\frac{F}{d^2} \qquad 1$$

where MH is the microhardness in *Pa*, d is the mean diagonal length of the projected impression in meters, F is the peak force in Newton and α is the included angle between two non adjacent faces (136° for the Vickers indenter).

Crystallization temperatures upon scanning at different heating rates and melting enthalpies were measured with a Perkin Elmer DSC7 fluxed with dry nitrogen and calibrated for temperature with indium on heating at 10°C/min.

Continuous Cooling Transformation (CCT) of PET

The CCT behavior of PET with reference to the phases formed has been examined in more detail in a previous work [2]. The dependence of density and microhardness on cooling rate shown in Fig. 1 evidences this continuous transformation. Far to the left, both density and microhardness show relatively slow changes with cooling rate. As the superimposed WAXS patterns indicate, the morphology of PET in this interval is characterized by a strong presence of the stable triclinic phase which continues to exist up to ca 2°C/s. Starting from ca 1°C/s the disappearance of this stable phase gets accelerated. The very sharp curve between 1 and 3°C/s suggests a very fast transformation. Following this, density tends to show only very small changes while the

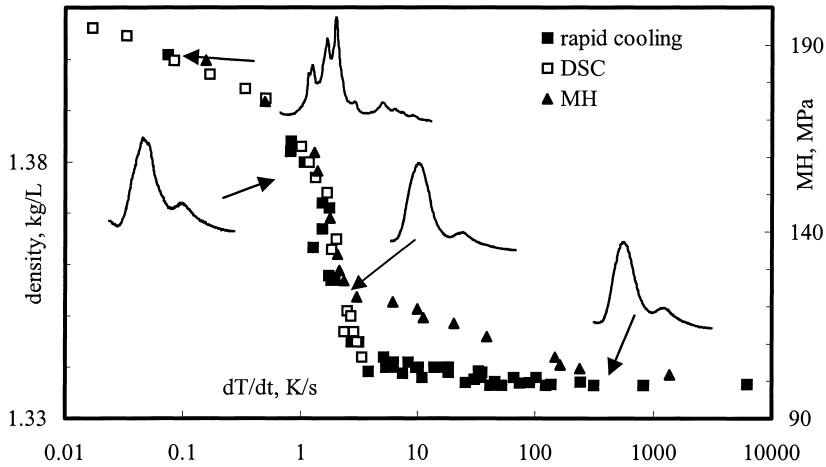

Figure 1 Density, microhardness and typical WAXD patterns of PET solidified by the CCT procedure and by DSC vs cooling rate.

more sensitive microhardness reveals the presence of an ongoing transformation which we believe to be associated with a size distribution of physical cross-links. In fact, after the disappearance of the triclinic phase, the polymer does not behave as a completely amorphous polymer. Figure 1 itself hints this incongruity. With changes in cooling rate there appear distinct differences in behavior between the respective samples. Therefore, this phase should not be identified as amorphous because the long period present and the crystallization enthalpy detected for cooling rates higher than 2°C/s [2] say the opposite. The WAXS spectra instead reveal the absence of crystallinity. That was why it was called as a pre-crystalline phase in the previous work.

In the following, the evolution of this concept towards the existence of physical cross-links will be justified by comparing the behavior of CCT samples during ageing and isothermal crystallization. It will thus be possible to confirm the existence of a size distribution of physical cross-links and its dependence on cooling rate.

A major evidence in this regard can be obtained from Fig. 2 where the dependence of density with crystallization time is compared for different samples melt solidified at different cooling rates (2, 6, 11, 20, 150 and 1500°C/s), all of them in the region where only the amorphous halo is observed from the WAXS patterns (see Fig. 1). The figure demonstrates how these apparently amorphous samples behave during isothermal crystallization from the glass at 100°C. It will not be difficult to note how the crystallization rate decreases with cooling rate by simply comparing the half times of

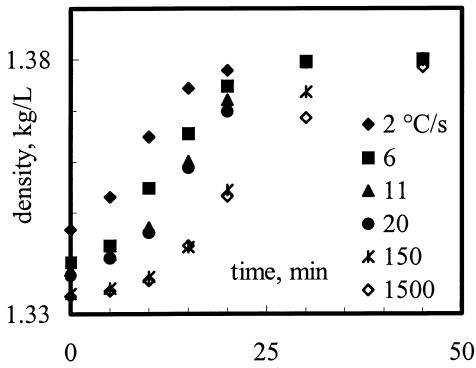

Figure 2 Isothermal crystallization of amorphous PET vs cooling rate. Density measured after holding for different times at 100°C.

crystallization. In fact, the rate of crystallization is seen to depend on the initial state of the quenched amorphous samples. A plausible explanation for this lies in the inherent difference in the sizes of physical cross-links. Some idea about their difference can be obtained by comparing their nucleation density which can be estimated by assuming that the mechanism of isothermal crystallization is the same for all the samples. Thus, for instance, the nucleation density of the 2°C/s sample is 2.3 times as much as that of the sample quenched at 100°C/s implying that crystallization in sample 2°C/s started on a larger population of nuclei than in sample 100°C/s [3]. However, this difference in nucleation density may not reflect the actual number of nuclei frozen in the samples during quenching. It may probably refer to the stable nuclei at the isothermal crystallization temperature, supposing that those physical cross-links smaller than the critical nuclei size should have rapidly dissolved. Thermodynamics also suggests that a distribution of sizes of physical cross-links exists below the equilibrium melting temperature. This means, when the sample is brought to the crystallization temperature those clusters with sizes greater than the critical dimensions will remain stable, whereas the others may cancel out. Without considering that the dynamics of this process may be in its turn influenced by the network structure of the physically cross-linked rubber.

Figure 3 compares the dependence of microhardness and WAXS patterns on density for the as-quenched and the isothermally crystallized samples. Note that the starting samples, whose crystallization kinetics is compared in Fig. 2, are restricted to the 'amorphous' interval as can be deduced from the superimposed WAXS patterns. Here, microhardness shows marked variations in a small interval of density. These changes in microhardness that are related to changes in internal order (precursors of the final crystalline state) suggest wide differences in the organizations of the latter[17].

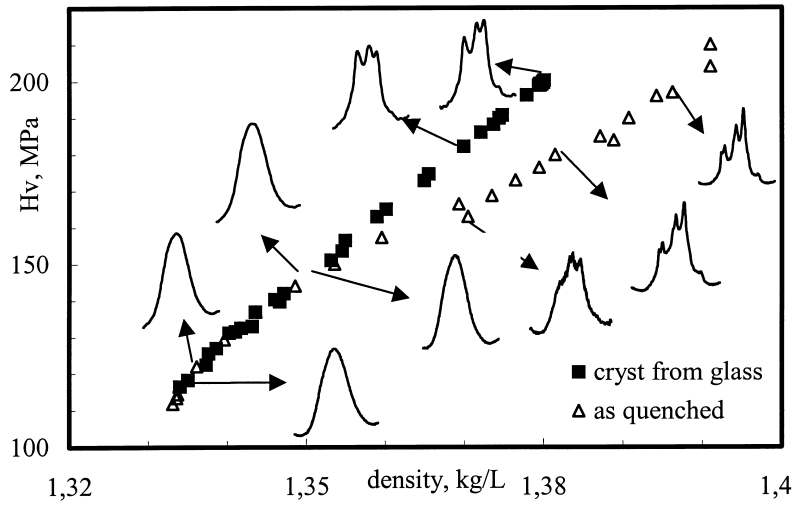

Figure 3 Microhardness dependence upon density for as quenched samples (open symbols) and after annealing at 100°C. Selected WAXS patterns are also shown for given conditions (see text).

An estimation of the critical radius of a nucleus, R*, at 100°C can be obtained from the relation:

$$R^* = 2\sigma * T^\circ / \Delta H / \Delta T \qquad 2$$

Where σ is the average surface energy at the crystal-amorphous boundary taken ($27 erg/cm^2$), T° is the equilibrium melting temperature (553°K) and ΔH is the enthalpy of crystallization ($1.8*109 erg/cm^3$). Assuming the respective values shown in parenthesis [18], a value of ~1 nm is obtained for the radius of nuclei of critical dimensions at 100°C.

Therefore, it is very likely that many of the physical cross-links that have contributed largely to the visible differences in microhardness seen in Fig. 1 have had sizes smaller than the critical dimensions at 100°C. So, they did not grow into nuclei. Probably some of them dissolved in the intervening amorphous phase while others got trapped due to the very low segmental diffusivity of the amorphous phase in the physically cross linked rubbery state. The higher microhardness values and less ordered WAXS patterns associated with the samples annealed at 100°C as compared to the as-quenched ones shown in Fig. 3 also support this argument. On the other side, since the material is a labile network above the T_g, physical cross-links larger than the critical size defined by eq. 2, may act as nuclei for crystallization. Therefore, it can be said that not all physical

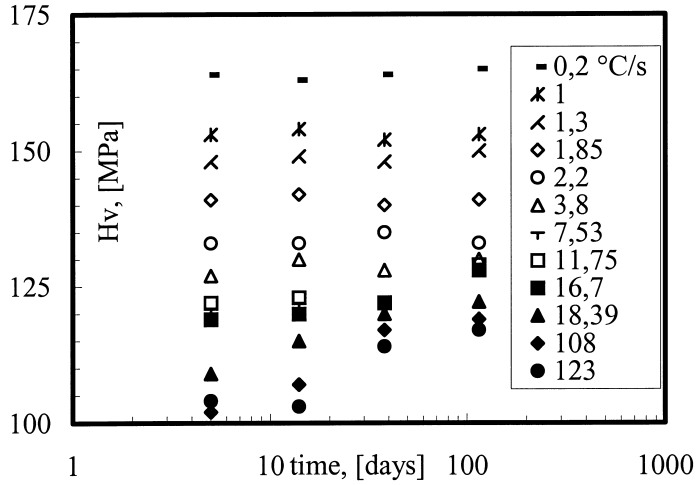

Figure 4 Room temperature ageing of PET monitored by microhardness as a function of initial cooling rate

cross-links transform into nuclei and the formation of stable physical cross-links is largely governed by the cooling rate.

The foregoing discussions have focused on the role of physical cross-links above the T_g. In the following sections instead it will be attempted to investigate and clarify the influence of physical cross-links on the behavior of glassy PET below the T_g.

Figure 4 shows the changes in microhardness during ageing at ambient temperature. As already pointed out in other works[19] the dependence of microhardness with ageing time is influenced by cooling rate. Thus, it is confirmed that for crystalline samples, i.e. for lower cooling rate samples (prepared with cooling rates less than 2°C/s) microhardness remains constant during ageing, the absolute values depending on cooling rate and therefore on crystallinity (see Fig. 1). For higher cooling rate samples that are all amorphous (>2°C/s) instead, microhardness increases with the logarithm of ageing time. Moreover, the results of Fig. 4 indicate that, for these samples, also the rate of increase in microhardness is a function of the initial cooling rate. Nevertheless, the differences in T_g between these samples are negligible. Therefore, the increase in microhardness with ageing time encountered with these amorphous samples cannot be solely ascribed to the free volume frozen during quenching.

On the other hand, the dependence of the rate of increase in microhardness on cooling rate observed in the amorphous samples implies that the ageing rate is a function of the

initial structure of these samples and therefore of the density of physical cross-links. Hence, the network structure generated by the onset of new physical cross-links should in this case act as a constraint for the amorphous solid limiting local mobility. This hypotheses may be plausible although it is not clear whether this is the only mechanism acting. If ageing indeed causes the onset of new physical cross-links, then this could be a joint mechanism for the increase in microhardness observed in the amorphous samples during ageing. Furthermore, this mechanism could also explain why the higher cooling rate samples of Fig. 4 do not show any asymptotic trend.

Results of rejuvenation test

In order to clarify the role of ageing on the onset of physical cross-links and compare it with the cross-links already determined during solidification, a rejuvenation procedure schematically shown in Fig. 5 was devised. The procedure was centered at following the evolution, at a temperature close to the T_g, of the macroscopic properties influenced by the density of physical cross-links of fresh and aged samples.

In Fig. 5, $dT/dt|_1$ refers to the CCT cooling rate with which a sample is prepared from the melt. T_{ag} and t_{ag} respectively stand for ageing temperature and time whenever a sample is subjected to ageing before rejuvenation. Rejuvenation is carried out by heating the sample (fresh or rejuvenated) to the rejuvenation temperature T_{rej}, rapidly (in about 10s), and keeping it at this temperature for different times, t_{rej}. The sample will be then cooled to room temperature at a constant rate $dT/dt|_2$. A non crystallizable polymer, PMMA, was also included in the study in order to compare the behavior of PET with that of an amorphous material. The ageing temperatures were about 35°C below T_g while rejuvenation was carried out at 10°C above T_g. The glass transition temperatures, as measured by DSC on freshly quenched samples, were 77 and

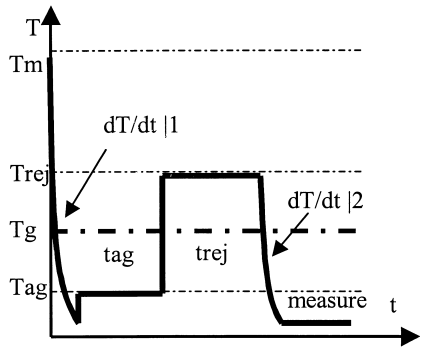

Figure 5 Rejuvenation procedure. Properties measured at room temperature.

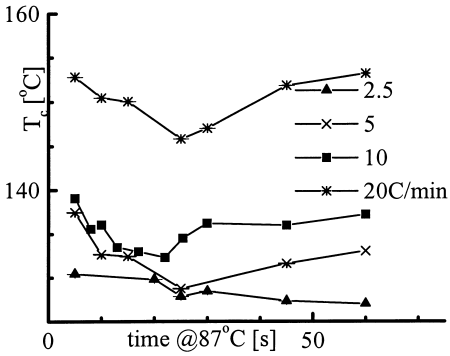

Figure 6 Temperature of maximum crystallization rate, T_c, for PET rejuvenated samples vs rejuvenation time, t_{rej}, at 87°C.

115°C for PET and PMMA respectively. At this point, however, it is good to note the experimental limitations of this procedure which can be clearly understood from the dispersion of the data collected and reported in the sections below. They probably derive from the cumulative propagation of errors due to the complex thermal treatment that the tested samples underwent.

Figure 6 reports the dependence of the maximum crystallization temperature, T_c, of a PET sample previously quenched at 100°C/s on rejuvenation time for different DSC heating rates. The figure shows that T_c assumes a minimum in many cases, the minimum becoming more marked with increasing DSC heating rate and tends to cancel out at the minimum heating rate adopted (2.5°C/min). In most cases the minimum is observed at t_{rej} of ca 25s. So, at a heating rate of 2.5°C/min the time spent above the T_g is relatively high that it cancels out the observed phenomenon. The minimum suggests the presence of two competitive phenomena both having time scales of few tens of seconds. On the other hand this decrease in T_c which is related to a faster crystallization kinetics may be attributed to an increase of physical cross-links. In addition, it can be observed from the same figure that such effect tends to cancel out on further increasing the time spent at 87°C since this temperature is above the T_g.

These observations are further confirmed by the relaxation enthalpy at the T_g of PET and PMMA samples rejuvenated after ageing as reported in Fig. 7. The figure shows that for aged sample 3800°C/s the relaxation enthalpy cancels out immediately upon rejuvenation similar to the aged PMMA sample while a residual relaxation enthalpy is observed for the aged sample 100°C/s. Although this residual enthalpy appears to be small, it is nevertheless higher than those of aged PET 3800°C/s and PMMA samples and does not seem to depend on rejuvenation time. The source of a residual enthalpy upon rejuvenation above T_g might be related to the onset of a rubbery phase in which

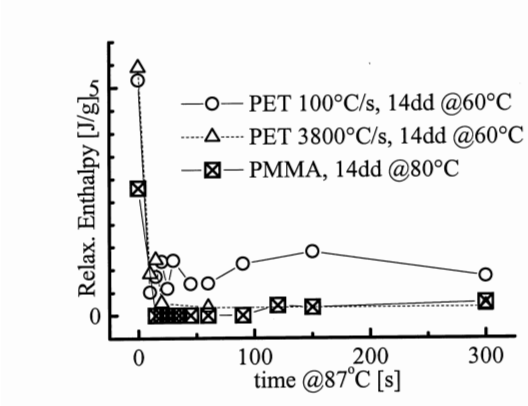

Figure 7 Relaxation enthalpy at the glass transition of aged PET and PMMA samples afterwards rejuvenated at 87 and 125°C respectively vs rejuvenation time, t_{rej}.

the excess enthalpy accumulated during ageing has not been released due to a constraint. In the light of this, the behavior of the aged PET sample 100°C/s can be attributed to the onset of a more constrained network as compared to the other samples. The similarity between the 3800°C/s PET and the PMMA samples suggests that for a PET quenched at such a high cooling rate (3800°C/s) there is a leveling off of the "effectiveness" of the physical cross-links eventually formed.

PMMA was here used as a "blank" for which it is implicitly assumed that the phenomena observed in PET and discussed in the introduction, i.e., the onset of physical cross-links, do not occur. In fact PMMA quenched samples do not show any time dependent phenomenon on rejuvenation as the comparison of the microhardness of rejuvenated fresh and aged samples could show. PMMA is therefore used in this context to compare the results obtained on rejuvenation of PET with a purely time dependent α relaxation process. This approach may look rather primitive, as it is difficult to exclude, even if the same degree of overheating (10°C above T_g) is used for the rejuvenation temperature, the possibility that these same processes could occur with a time scale outside the window of these experiments. To our knowledge however there are many instances justifying the assumption of PMMA as a blank in this context: it is non crystallizable although it is a flexible chain polymer, it has a bulky side group and it is a brittle material below T_g.

The rejuvenation tests made at 87°C indicate that there exist differences in cross-link density between samples 100 and 3800°C/s. In addition, isothermal crystallization tests made at a higher temperature (100°C) reveal that for 100°C/s and above the crystallization rate remains constant suggesting that the size distribution of physical cross-links of samples prepared at a cooling rate of 100°C/s and above does not add any

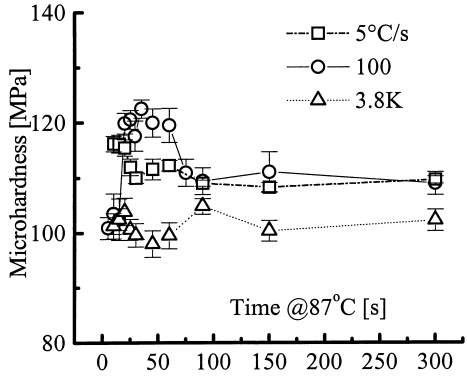

Figure 8 Influence of cooling rate on time of rejuvenation dependence, t_{rej}, of microhardness of PET samples.

contribution to the nucleation density. It could also be shown [3] that upon increasing crystallization temperature the differences between crystallization half times of amorphous samples quenched at different cooling rates become even smaller than those pointed out in Fig. 2 for 100°C. This observation implies that although physical cross-links may be generated even at very high cooling rates, their stability however decreases (i.e. decrease in size) as the cooling rate is increased.

It has been said that for the aged sample 100°C/s, physical cross-links stabilize the relaxation enthalpy through the onset of a network structure. The network is apparently stable at the rejuvenation temperature although larger temperatures may possibly affect its stability. The following sections on the other hand can offer further experimental evidence to clarify whether the network is generated by the ageing process or it is preliminary to it.

Figs. 8 and 9, respectively, report the changes in microhardness with rejuvenation time in dependence on cooling rate for fresh and aged PET samples. From Fig. 8, it can be observed that the microhardness associated with the fresh sample 3800°C/s does not seem to be affected by rejuvenation and shows the minimum asymptotic value as compared to the other two. The presence of the maximum in microhardness for the fresh sample 100°C/s instead shows clearly its dependence on rejuvenation time. The microhardness of the fresh sample 5°C/s also tends to decrease with rejuvenation time.

Figure 9 on the other hand reveals that after the introduction of ageing the maxima disappears and the microhardness decreases from an initially much larger value with respect to the freshly quenched samples. This implies that ageing has modified the morphology by introducing new physical cross-links: microhardness again decreases with initial cooling rate although it is now markedly higher for the 5 and 100°C/s

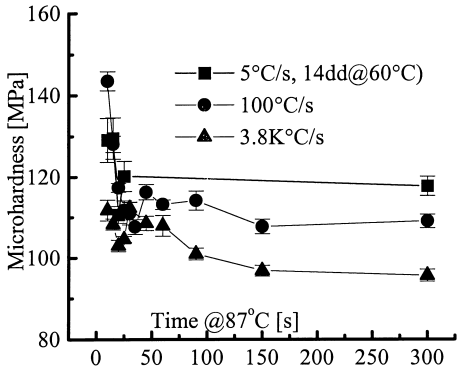

Figure 9 Influence of cooling rate on time of rejuvenation dependence, t_{rej}, of microhardness of PET aged samples.

samples with respect to the 3800°C/s sample. When rejuvenated, the aged samples show a rather fast settling towards the asymptotic values. In particular for sample 3800°C/s, a slight decrease of microhardness with rejuvenation time takes place before reaching the plateau. However, the introduction of ageing has not altered the asymptotic values of samples 100 and 3800°C/s. Aged sample 5°C/s instead seems to assume a slightly higher asymptotic value with respect to the fresh. In conclusion the asymptotic values decrease with increasing cooling rate.

Additional experimental evidence can be obtained from the density dependence on rejuvenation time of fresh and aged samples shown in Fig. 10. As indicated in this figure, it is evident that the samples analyzed this time are prepared with different cooling rates and rejuvenated at a slightly higher temperature (3°C higher than the one used so far). However, if one makes reference to Fig. 1 and to the pertinent cooling rate window, the similarity in behavior between these and the former samples which is dependent on initial "state", i.e. on initial cooling rate, can be recognized immediately. This is worth to emphasize since it confirms that the CCT approach allows to identify the influence of cooling rate on the morphology developed.

In Fig. 10 the dependence of density (measured at room temperature) of two samples quenched at ca 2 and 200°C/s on rejuvenation time is compared with the behavior of the same samples after ageing at room temperature. The figure shows that the density of aged samples first increases rapidly with rejuvenation time and then decreases at a slower pace to a final value a little less than the initial. Because the samples are aged, it can be expected that the density should decrease when cooperative motions set in. Although it happened at long times, the decrease is also evident in the present case. In the case of the fresh samples, only the slowly quenched sample (2°C/s) shows the

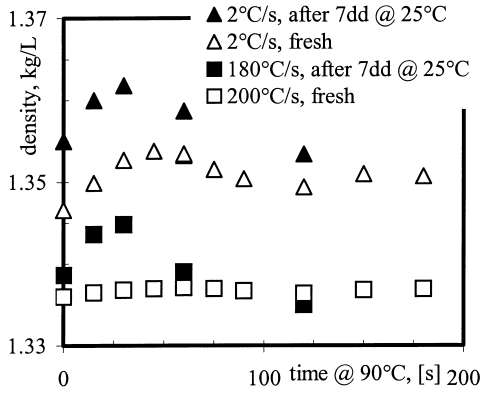

Figure 10 Influence of cooling rate and ageing on time of rejuvenation dependence, t_{rej}, of density of PET samples.

maximum in density while the density of sample 200°C/s immediately attains the equilibrium value at 90°C. This behavior when compared with the results already discussed makes the role of physical cross-links still clearer.

Physical cross-links acting as nodes form a networked structure in the amorphous matrix. So, during rejuvenation a sudden entropic recoil on these nodes eventually accompanied by the onset of cooperative motions takes place. It is probably this entropic recoil that is responsible for the density rise. In other words, the material behaves as a rubber before the maximum and it collapses upon releasing the excess free volume. It is plausible to say that on further increasing the rejuvenation time, a slow process of dissolution of clusters, controlled by size distribution and thermodynamics, develops.

Hence, on this basis, it is possible to give a tentative interpretation about the behavior of T_c and microhardness, respectively shown in Fig. 4 and Fig. 7, for the fresh sample cooled at 100°C/s. The minimum in T_c and the maximum in microhardness cannot be explained only by a decrease of free volume. T_c decreases when the number of nuclei increases. Therefore, before the maximum occurs the onset of new physical cross-links is favored by the decrease of constraints and by the local mobility associated with the release of the excess free volume frozen during quenching. In addition, the absence of the maximum in microhardness observed in Fig. 8 for the 100°C/s aged sample, confirms this interpretation. In this case, in contrast to the fresh sample, ageing has already given rise to a decrease of free volume and therefore a decrease of mobility. Therefore the behavior observed on the fresh 100°C/s sample in Fig. 7 for microhardness (maximum) and in Fig. 4 for T_c (minimum) is based on the same mechanism. However, it is probable that a contribution to the maximum of microhardness may also be due to the decrease of free volume, as Fig. 9 suggests.

These results confirm that the size of physical cross-links (and may be their number) is affected by cooling rate as well as by ageing. The relationship between cooling rate and ageing is also qualitatively clear. If cooling rate is low, the network structure will be immobilized by the bigger size (stability) and possibly by the higher density of physical cross-links. In this case, ageing will affect mostly the stability of those already set in. This is evidenced in Fig. 8 where rejuvenation of the aged sample 5°C/s clearly shows an increase of the asymptotic microhardness with respect to the fresh one. At intermediate cooling rates, since the network is looser, new cross-links can be generated. They are however smaller and unstable and hence will be cancelled at the rejuvenation temperature. At even higher cooling rates, for instance the fresh 3800°C/s sample, the initial density and size distribution of cross-links is very small and the trend observed for the 100°C/s sample takes place in a much shorter time window not experimentally accessible. Therefore, for fresh samples in the cooling rate window of thousands of °C/s physical cross-links are mostly generated during ageing. That this is indeed the case is shown by the similarity of the microhardness of the 3800°C/s aged sample where a faint maximum vs. rejuvenation time is observed similar to the fresh 100°C/s sample. This is also confirmed by the influence of ageing on crystallization from the glass, already observed by other authors [14,15]. Although the cooling rate adopted for quenching was not specified, their samples should have been severely quenched with cooling rates above 1000°C/s.

Conclusions

For cooling rates above 2°C/s, solidification of PET from the melt by a Continuous Cooling Transformation (CCT) gives rise to physical cross-links dispersed in the amorphous phase. Although the mechanism of the onset of physical cross-links is not clear, it is nevertheless possible to freeze the morphology at the stage where the underlying mesomorphic structure, precursor of the crystallization process [20], is formed. Besides, the results have shown that the resulting physical network determines the properties of the material below and above the T_g. The network is not stable above T_g since physical cross-links may eventually dissolve due to the onset of cooperative motions. The results also suggest that a distribution of physical cross-links arises, the distribution being strictly dependent on the cooling rate. Their stability is determined by size effects and the temperature to which they are exposed. Some physical cross-links

may be stable well above the glass transition and act as nuclei for further crystallization from the glass depending on cooling rate. Upon decreasing cooling rate the stability of an increasing number of physical cross-links is enhanced.

Below the T_g, the process of ageing is largely governed by cooling rate and therefore by physical cross-links. The excess free volume normally frozen during quenching may also favor local mobility and the onset of further cross-links. However, the network structure formed during quenching can act as a constraint for large scale motion. As a result, only small new physical cross-links that become less stable upon rejuvenation will be formed. Therefore, the stability of physical cross-links formed during ageing also depends on cooling rate: for high cooling rates constraints decrease and size distribution of physical cross-links formed during ageing should increase.

Extending the discussion, the mechanism invoked for the onset of physical cross-links can be hypothesized as a precursor to the nucleation stage, i.e. nucleation takes place by local molecular arrangements, similar to the onset of physical cross-links described here for PET. If so, then the lower thermal kinetic boundary for nucleation should be identified. Often, in crystallization kinetics modeling, the limiting lower temperature boundary for molecular diffusion has been considered to be the T_g as it is associated with the freezing of the segmental chain mobility involved in cooperative motion. However, if a precrystalline order is first established in crystallization as suggested recently, [20] one should rather consider the β transition temperature at which all the elementary motions get frozen as the lower thermal kinetic boundary.

The mechanism of dissolution of physical cross-links is slow and it depends on the departure of the size distribution of the physical cross-links from equilibrium. The dissolution process is also constrained by the physical cross-links themselves. So, during processing the onset of physical cross-links may significantly affect crystallization of PET from the glassy state. The influence of initial structure on crystallization from the glass cannot be explained only in terms of differences in nucleation density as this would be of minor entity as discussed previously. The network structure should have a major role, especially for fast processing, on the stress level the network is able to withstand, thus influencing significantly orientation and in turn flow induced crystallization.

Acknowledgements

This work has been supported by EU BRITE project "Decrypo" contract BRPR.CT96.0147 and by the Italian Ministry of University PRIN99. E.V. gratefully acknowledges a fellowship from Consiglio Nazionale delle Ricerche, Italy.

[1] Piccarolo S., *J. of Macrom. Sci., Physics*; **1992**, *B31*, 501.
[2] Piccarolo S., V. Brucato, Z. Kiflie; *Polym. Eng. &* Sci. **2000,** *40*, 1263.
[3] Kiflie Z., S. Piccarolo, V. Brucato, F. J. Baltà-Calleja; "Role of Thermal History on Quiescent Cold Crystallization of PET"; Polymer, submitted.
[4] Pereira J. R. C., R. S. Porter; *J. Polym Sci. Polym. Phys.,* **1983**, *21*, 1133.
[5] Auriemma F., P. Corradini, C. De Rosa, G. Guerra, V. Petraccone, R. Bianchi, G. Di Dino, *Macromolecules*, **1992**, *25*, 2490.
[6] Yeh G. S. Y., P. H. Geil, *J. Macromol. Sci.,* Phys., **1967**, *B1*, 235.
[7] Wunderlich B., I. Okazaki, *J. Thermal Analysis*, **1997**, *49*, 57.
[8] Song, M.; Hourston, D. J.; *J. of Thermal Anal. & Calorim.*; **1998**, *54*, 651
[9] Schick C; A Wurm; A. Mohamed; *Colloid & Pol. Sci.*; **2001**, *279*, 800
[10] Imai M., K. Kaji, T. Kanaya, Y. Sakai, *Phys. Rev.*, **1995**, *B52*, 12696.
[11] Shimada T., M. Doi; K. Okano, *J. Chem. Phys.,* **1988**, *88*, 7181.
[12] Fukao K., Y. Miyamoto, *Physical-Review-letters*, **1997**, *79*, 4613.
[13] Wang Y.; D. Y. Shen, R. Y. Qian, *J. Pol. Sci/B Pol. Phys.*, **1998**, *36*, 783.
[14] Bove L., C. D'Aniello, G. Corrasi, L. Guadagno, V. Vittoria, *Polymer Bulletin*, **1997**, *38*, 579.
[15] McGonigle E. A., J. H. Daly, S. Gallagher, S. D. Jenkins, J. J. Liggat, I. Olsson, R.. A. Pethrick, *Polymer*, **1999**, *40*, 4977.
[16] Brucato V., S. Piccarolo, V. La Carrubba, "An Experimental methodology to study polymer crystallization under processing conditions. The influence of high cooling rates", *Chem. Eng. Sci.*, submitted
[17] Baltà-Calleja F.J., M. Cruz Garcia, D. R. Rueda, S. Piccarolo, *Polymer*; **2000**, *41*, 4143.
[18] Ziabicki, A.; *Colloid Polym. Sci.*, **1996,** *274*, 705
[19] Ania F., J. Martinez Salazar, F.J. Baltà-Calleja; J. Mater. Sci.; **1989**, *24*, 2934
[20] Strobl G.; *Eur. Phys. J. E*, **2000**, *3*,165.